International Journal of Fluid Power 8 (2007) No. 2 pp. 17-24

REDUCING INFLUENCE OF ECCENTRIC LOAD ON DYNAMIC CHARACTERISTICS OF ROTARY ACTUATOR

Ye Qian and Meng GuoXiang

SMC pneumatic technical Center, Mechanical Engineering School, Shanghai Jiao Tong University, Dong Chuan road 800, Min Hang district, Shanghai, China, 200240
yeqian@sjtu.edu.cn, gxmeng@smcjp.co.jp

Abstract

The main objective of this study is to reduce the eccentric load's influence on the dynamic characteristics of a horizontally installed rotary actuator. The solution is drilling a hole into the rotary shaft of a rotary cylinder. With the rotation of the rotary actuator the hole will open and connect the two working chambers within a certain angular range, the back pressure will increase and the torque introduced by the back pressure partly compensates for the torque of the eccentric load. The design procedure for the connecting hole is as follows: First, experiments that study the effect of eccentric loads on the dynamic characteristics of a rotary actuator were carried out, and a stability index α_v was proposed; Second, a mathematical model including the connecting hole was built; Third, a real–coded GA optimization design for the connecting hole whose object is to minimize α_v was conducted. Simulations and test results show that the method worked efficiently.

Keywords: pneumatic rotary actuator, eccentric load, instability, real-coded genetic algorithm, optimization design

1 Introduction

A pneumatic rotary actuator is a kind of pneumatic actuator which can revolve to and from less than 360˚. It transforms the pressure energy of compressible gas into mechanical energy and generates driving torque to rotate the work-piece (Zhang, 2003). Pneumatic rotary actuators are widely used in the displacement, overturn, classification, clamping, opening and closing of a valve, driving a robot arm etc. (Yusimitsu, 2004; Yamato, 2004). Among the applications, rotary actuators with eccentric loads are frequently used.

In this paper a series of experiments studying the effect of eccentric loads on the dynamic characteristics of rotary actuators were conducted. It was found that the angular acceleration curve of a pneumatic rotary actuator mounted horizontally has a distinguishing dual hump-shaped feature due to the presence of an eccentric load (Ye, 2006). It can be called an instability phenomenon. The phenomenon will lead to a sharp increase in the inertia energy exerted on the revolving shaft. Over time, the shaft will yield and break down (Li, 1991). It has a significant influence on the rotary actuator life and the positioning accuracy of controlled devices such as robot arms. The study addresses the problem and research has been carried out to find a simple way to suppress the influence of eccentric loads on the motion of rotary cylinders and an easy method to modify the rotary cylinder.

During the study a solution was found of drilling a connecting hole into the shaft of the rotary cylinder to connect one working chamber with the other within a rotary angle range. With the rotation of the rotary actuator the hole will open and connect the two working chambers within a certain range of angles, the back pressure will rise and the torque introduced by the back pressure partly compensates for the torque of the eccentric load. The design procedure for the connecting hole is as follows: First, based on the experimental results of studying the effect of eccentric loads on the dynamic characteristics of a rotary actuator a stability index α_v is proposed; Second, a mathematical model including the connecting hole was built; Third, a real–coded GA optimization design for the connecting hole whose object is to minimize α_v was conducted. Simulations and test results show that the method solved effectively the instability problem of a rotary cylinder with eccentric loads.

This manuscript was received on 24 January 2007 and was accepted after revision for publication on 24 May 2007

2 Instability Phenomenon and Instability Index α_v

2.1 Instability Experiments and Results

A test stand (Fig. 1) was built to study the effect of eccentric loads on the dynamic characteristics of rotary actuators. The test stand mainly consists of an air source, solenoid valve, pneumatic rotary actuator, angular sensor, pressure sensor and eccentric load. One side of the shaft of the actuator connects with the eccentric load and the other side connects with the angular sensor measuring the angular position. The rotary actuator being tested has two pairs of ports, one pair of ports connected with the solenoid valve and the other connected to the two pressure transducers. Two pressure sensors connect with two chambers respectively which measure the chambers' instantaneous pressure. The solenoid valve connects the air source and the two chambers of the actuator which control the direction of motion of the rotary actuator. Two pressure signals p_1, p_2 and one angular signal θ were sampled by the computer through the A/D module of one data acquisition card (DAC). The DO module of the DAC controlled the on-off of the solenoid valve. During the experiments the moment of inertia remains the same and only the maximum eccentric load torques change due to different eccentric loads. The angular velocity ω and acceleration γ signals are obtained from first and second derivatives of the angular position signal θ. The size of the rotary actuator is 50 mm. The initial position of the rotary actuator is 0°, and the mount position of the eccentric load is also 0°. The total rotary angle of the rotary actuator is 270°.

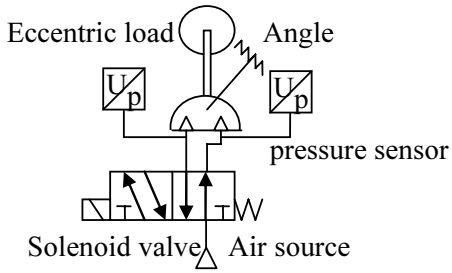

Fig. 1: *The test-bed schematic of the rotary cylinder velocity stability*

2.2 Experiments and Discussions

Figures 2 through 4 show experimental results of the dynamic characteristics of a rotary actuator under a supply pressure of 0.2 MPa with different maximum eccentric load torques.

As shown in Fig. 2, Fig. 3 and Fig. 4, the instability of the rotary actuator is caused by the presence of eccentric loads and regardless of the presence of an eccentric load on the rotary actuator, the angular acceleration curves show two hump-shaped forms. In other words, the curve has two local maximum values (two hump values). In this paper α'_{max} denotes the first local maximum and α_{max} denotes the second local maximum. These values can be obtained by finding the local maximum values of the angular acceleration test results. In Fig. 2 there is no eccentric load torque exerted on the shaft but the acceleration curve still has two hump-shaped forms. The possible reason is that the rotary actuator has one vane and the vane serves as an eccentric load.

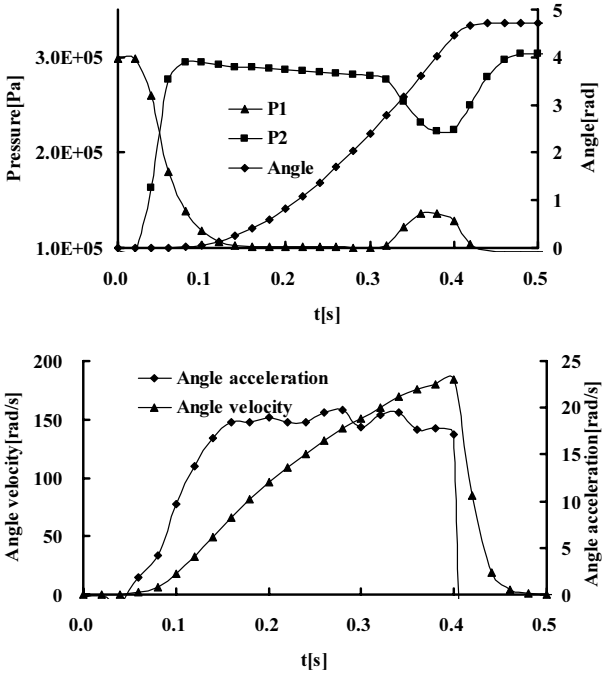

Fig. 2: *The test curves of the dynamic properties of the rotary actuator (M_{ec} = 0 Nm)*

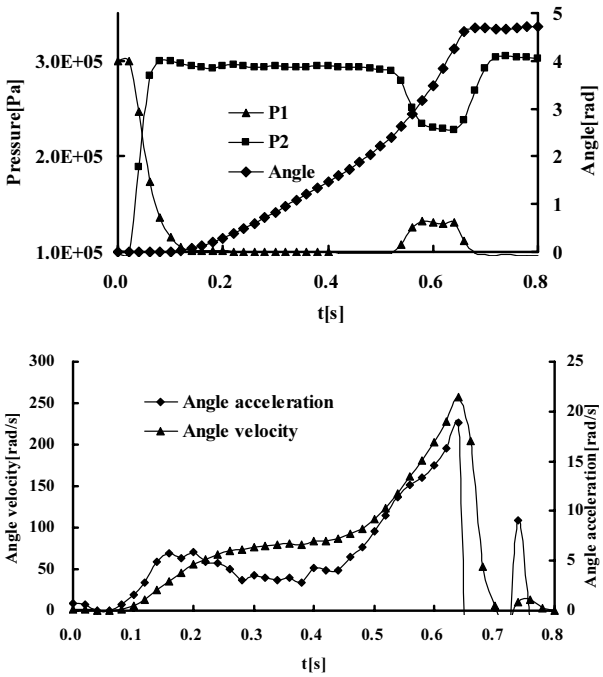

Fig. 3: *The test curves of the dynamic properties of the rotary actuator (M_{ec} = 1.09 Nm)*

Comparing Fig. 2, Fig. 3, and Fig. 4 it can be seen clearly that the ratio of α_{max} to α'_{max} increases as the maximum eccentric load torque increases. A physical quantity to represent the degree of instability has been found and is called the instability index. The stability

index α_v is here defined as the ratio of α_{max} to α'_{max}. When the value of α_v is close to 1, the rotary actuator's angular acceleration is stable (Fig. 2). The larger the difference between α_v and 1, the more unstable the actuator's acceleration becomes (Fig. 3, Fig. 4).

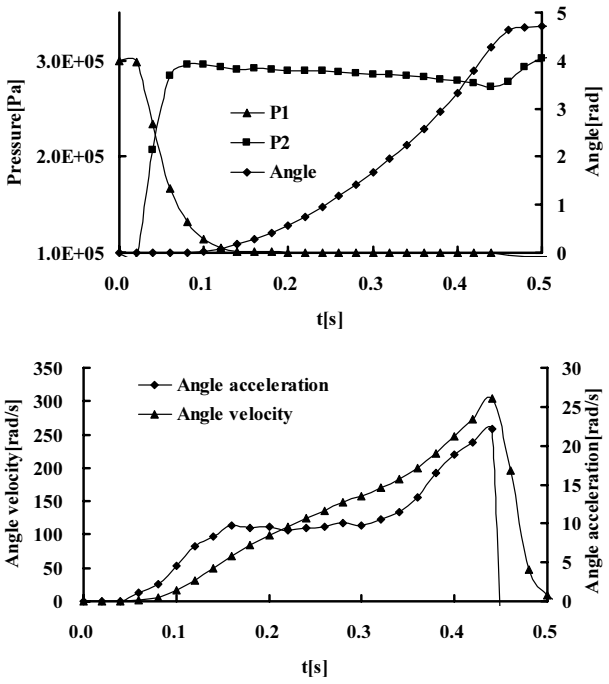

Fig. 4: *The test curves of the dynamic properties of the rotary actuator (M_{ec} = 2.18 Nm)*

It is easy to use control systems to settle such questions (Wang P., 2003; 2004), however, this is costly and complicated. If a hole is drilled into the shaft of the rotary cylinder, as the rotary actuator rotates the hole will open and connect the two working chambers within a certain range of angles, the back pressure will rise and the torque introduced by the back pressure partly compensates for the torque of the eccentric load. This solution is maybe the easiest way to solve the instability question.

3 Mathematical Model of a Pneumatic Rotary Actuator with Connecting Hole

The dynamic characteristics of pneumatic rotary actuators can be described by the following equations:

- Pressure differential equations of the two chambers
- Pressure-mass flow rate equations of the solenoid valve
- Torque equilibrium equation of the rotary shaft
- Mass flow rate equation of the connecting hole

In the following model some assumptions are made:

- ideal gas;
- constant supply pressure p_s and temperature T_s;
- exhaust pressure equals the environment pressure;
- gas flowing through the valve ports and other throttles are isentropic processes;
- spatially averaged temperature inside the chambers and processes are in local equilibrium;
- spatially averaged properties at the chambers' ports;
- negligible kinetic terms in the energy equations;
- constant ambient conditions.

The model does not consider:

- leakages between the chambers and between chambers and the external environment;
- resistive, inductive, capacitive and propagation effects in the pipes;
- the influence of the pipe connections on the actuator inlets;

3.1 Pressure Differential Equations of the Two Chambers

Figure 5 illustrates the schematic diagram of the rotary actuator transmission system with an eccentric load.

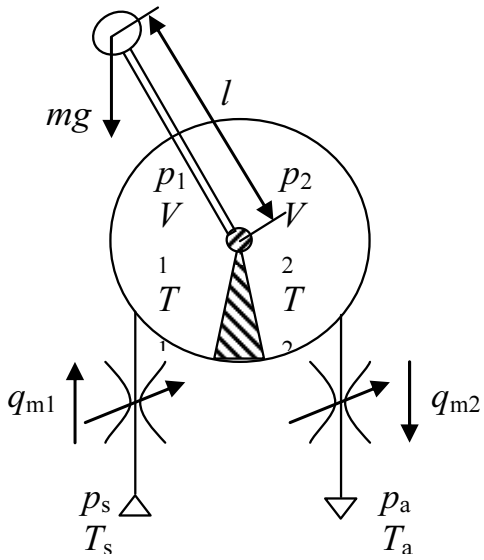

Fig. 5: *Schematic diagram of the rotary actuator transmission system with eccentric load*

Under the conditions mentioned above, for chamber 1 (inlet chamber), the energy equation, Eq. 1, describing the adiabatic charging process of constant air supply pressure to a finite chamber (Wang, 2003) is

$$kRT_1 dm_1 = V_1 dp_1 + kp_1 dV_1 \tag{1}$$

The charging mass flow rate equation can be described as:

$$q_{m1} = \frac{dm_1}{dt} \tag{2}$$

Substituting Eq. 2 into Eq. 1, the following expression is obtained:

$$\frac{dp_1}{dt} = \frac{kRT_1 q_{m1}}{V_1} - \frac{kp_1}{V_1}\frac{dV_1}{dt} \tag{3}$$

During the charging process, the absolute temperature in the chamber T_1 should be (Zhang, 2003):

$$T_1 = \frac{kT_s}{1+(k-1)\left(\frac{p_a}{p_1}\right)} \tag{4}$$

For chamber 2 (outlet chamber), the energy equation, Eq. 5, describing the adiabatic discharging process of a finite chamber to atmosphere is

$$-kRT_2 dm_2 = V_2 dp_2 + kp_2 dV_2 \tag{5}$$

The discharging mass flow rate equation can be described as:

$$q_{m2} = -\frac{dm_2}{dt} \tag{6}$$

Substituting Eq. 5 into Eq. 6, the following expression is obtained:

$$\frac{dp_2}{dt} = \frac{kRT_2 q_{m2}}{V_2} - \frac{kp_2}{V_2}\frac{dV_2}{dt} \tag{7}$$

During discharging process, the absolute temperature in the chamber T_2 should be (Zhang, 2003):

$$T_2 = T_a \left(\frac{p_2}{p_s}\right)^{\frac{k-1}{k}} \tag{8}$$

The volume of the charging chamber of the rotary cylinder is:

$$V = A\theta \tag{9}$$

in which $A = b\dfrac{D^2 - d^2}{8}$.

Allowing for the dead volume, the volume of the two chambers can be described as:

$$V_1 = V_{1b} + A\theta = A(\theta_{1b} + \theta) = A\theta_1 \tag{10}$$

$$V_2 = A(\theta_{2b} + S - \theta) = A\theta_2 \tag{11}$$

Substituting Eq. 10 and Eq. 11 into Eq. 3 and Eq. 7 respectively yields:

$$\frac{dp_1}{dt} = \frac{kRT_1 q_{m1}}{A\theta_1} - \frac{kp_1}{\theta_1}\frac{d\theta}{dt} \tag{12}$$

$$\frac{dp_2}{dt} = \frac{kRT_2 q_{m2}}{A\theta_2} + \frac{kp_2}{\theta_2}\frac{d\theta}{dt} \tag{13}$$

3.2 Pressure-mass Flow Rate Equations of the Solenoid Valve

The equations used to describe the flow-rate characteristics of the valve behavior agree with ISO 6358. The mass flow rate entering chamber 1 is:

$$q_{m1} = \begin{cases} C_1 p_s \rho_0 \sqrt{\dfrac{T_0}{T_s}} & 0 \le \dfrac{p_1}{p_s} \le b_1 \\ C_2 p_s \rho_0 \sqrt{\dfrac{T_0}{T_s}} \sqrt{1 - \left(\dfrac{\frac{p_1}{p_s} - b_1}{1 - b_1}\right)^2} & b_1 \le \dfrac{p_1}{p_s} \le 1 \end{cases} \tag{14}$$

The mass flow rate entering chamber 2 is:

$$q_{m2} = \begin{cases} C_2 p_2 \rho_0 \sqrt{\dfrac{T_0}{T_2}} & 0 \le \dfrac{p_a}{p_2} \le b_2 \\ C_2 p_2 \rho_0 \sqrt{\dfrac{T_0}{T_2}} \sqrt{1 - \left(\dfrac{\frac{p_a}{p_2} - b_2}{1 - b_2}\right)^2} & b_2 \le \dfrac{p_a}{p_2} \le 1 \end{cases} \tag{15}$$

3.3 Torque Equilibrium Equation of the Rotary Shaft

The torque equilibrium equation of the rotary shaft is:

$$J\frac{d^2\theta}{dt^2} = A(p_1 - p_2) - k_w r^2 \frac{d\theta}{dt} \pm M - M_{ec} \tag{16}$$

The eccentric load torque equation is derived from Fig. 6.

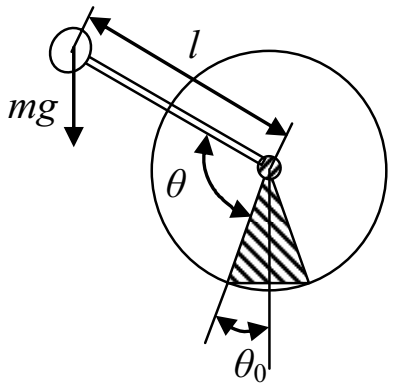

Fig. 6: *The computation diagram of the eccentric load*

$$M_{ec} = mgl\sin(\theta - \theta_0) \tag{17}$$

3.4 Mass Flow Rate Equation of the Connecting Hole

Compared with the original mathematical model of the pneumatic rotary cylinder, an additional mass flow rate equation for the connecting hole is presented:

$$q_{mh} = \begin{cases} C_h p_1 \rho_0 \sqrt{\dfrac{T_0}{T_1}}\varphi(\sigma) & \theta_o \le \theta \le \theta_c \\ 0 & \text{others} \end{cases} \tag{18}$$

$$\varphi(\sigma) = \begin{cases} 1 & 0 \le \sigma = \dfrac{p_1}{p_s} \le b_h \\ \sqrt{1 - \left(\dfrac{\sigma - b_h}{1 - b_h}\right)^2} & b_h \le \sigma = \dfrac{p_1}{p_s} \le 1 \end{cases} \tag{19}$$

When the chambers are connected with each other by the connecting hole, due to the pressure difference, some air in the charging chamber will enter the discharging chamber. Equation 12 thus changes to the following form:

$$\frac{dp_1}{dt} = \frac{kRT_1(q_{m1} - q_{mh})}{A\theta_1} - \frac{kp_1}{\theta_1}\frac{d\theta}{dt} \tag{20}$$

Equation 13 changes to:

$$\frac{dp_2}{dt} = \frac{kRT_2(q_{m2} - q_{mh})}{A\theta_2} + \frac{kp_2}{\theta_2}\frac{d\theta}{dt} \tag{21}$$

Equations 16 through 21 represent the mathematical model of a pneumatic angular actuator with a connecting hole. The dynamic characteristics of a pneumatic rotary actuator can be obtained by solving the group of differential equations in MATLAB using the Runge-Kutta method.

4 Optimization Design for the Connecting Hole

After establishing the mathematical model of a rotary actuator with a connecting hole, the optimization design is carried out for the connecting hole whose purpose is to discover the best combination of the connecting hole sonic conductance C_h, opening angle θ_o and closing angle θ_c to minimize the speed stability index mentioned above. Here the real-coded genetic algorithm is used to implement the optimization design.

4.1 Range of Optimization Design Parameter

Table 1 illustrates the simulation parameters of the rotary actuator transmission system.

Table 1: Simulation parameters of the rotary actuator transmission system

Simulation parameters		value
inlet	C_1	1.3e-8
	b_1	0.33
outlet	C_2	1.6e-8
	b_2	0.32
l_t (m)		0.3
d_t (mm)		4
D (mm)		58
d (mm)		25
h (mm)		40
m (kg)		0.74
J (kg m^2)		0.0167
l (mm)		75
m_y (kg)		0.65
l_y (mm)		22
p_s (MPa)		0.2, 0.3, 0.5
S (rad)		4.71
M_{ec} (Nm)		2.18

Table 2 illustrates the span of optimization design parameters. Because the critical pressure ratio of the connecting hole is unknown, $b_h = 0.3$ is used instead, and it is a reasonable value.

Table 2: Table of optimum design parameter span

Optimization variables	range
C_h	0.1~10
θ_o	0~4.71
θ_c	0~4.71

4.2 Optimization Object and Constraints

The optimizing object chosen here is to minimize the rotary cylinder speed stability criterion α_v, namely $\min(\alpha_v)$.

The constraint conditions are:

- The rotary actuator must fulfill the full stroke in a fixed time (no cushion).
- The opening angle of the connecting hole θ_o should be less than the closing angle θ_c.

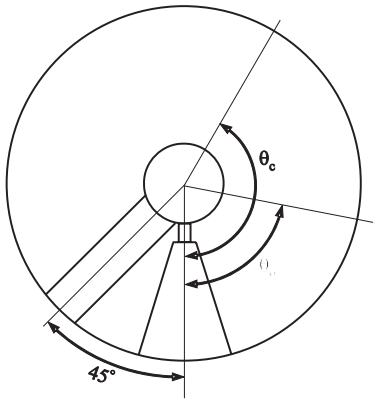

Fig. 7: *The relationship between θ_o and θ_c*

To assure that the design of the hole has a similar effect on the return motion, θ_o and θ_c have the following relationship:

$$\theta_c = \frac{3\pi}{2} - \theta_o \tag{22}$$

The two constraint conditions can be described as follows:

$$\theta(t_e) = S \tag{23}$$

$$\theta_o \le \theta_c \tag{24}$$

So the optimization object function will be:

$$\left.\begin{aligned} \min \quad & f(C_h, \theta_o, \theta_c) = \alpha_v \\ s.t. \quad & \theta(t_s) = S \\ & \theta_o \le \theta_c \end{aligned}\right\} \tag{25}$$

It is an optimization question with inequality constraint and it can be solved by using a penalty function method which converts the above into the unconstrained optimization question below (Wang L., 2003):

$$\left.\begin{aligned} \min F_p(C_h, \theta_o, \theta_c) &= \alpha_v + P(C_h, \theta_o, \theta_c) \\ P(C_h, \theta_o, \theta_c) &= \alpha\left(S - \theta(t_e)\right) + \beta\left|\min(0, \theta_c - \theta_o)\right| \end{aligned}\right\} \tag{26}$$

where P(X) is the penalty function and α and β are penalty factors. Because getting the minimum solution value belongs to the minimization question, the object function should be converted into a fitness function as follows:

$$F(X) = \left[F_p(X)_{\max} + F_p(X)_{\min}\right] - F_p(X) \tag{27}$$

where $F_p(X)_{max}$ and $F_p(X)_{min}$ stand for the maximum and minimum value of the object function in all individuals of every population separately and thus Eq. 25 has changed into a maximum optimization question.

4.3 Selection of Encoded Mode

The encoded modes often used are binary and real number (decimal) encoded modes. There are some insurmountable drawbacks for binary encoded modes. For example, it can not reflect the architectural feature of the solving question directly and has mapping errors. Furthermore, it may have Hamming cliffs problem. If higher accuracy is required, the string length must be increased, which decreases the algorithm efficiency and it is difficult for gene strings to understand before decoding. But these problems are not associated with the real encoded mode, so the real coded GA was chosen for this article.

4.4 Evolution Strategy

Here variable variation probability, crossover probability and elite selection method are selected as the evolution strategy. Individual number in a population is 20 and the stop criterion is the maximum reproduction generation and should be less than 500.

4.5 Algorithm Implementation

The genetic algorithm toolbox, which is popular in project design areas, was used to do the optimization design. In addition, the genetic algorithm toolbox's simulation environment was used to verify the results.

The optimum design result is the following. When the maximum eccentric load torque M_{ec} is 2.18 Nm and the air supply pressure is 0.4 MPa, θ_o = 0.5548 rad, θ_c = 4.1552 rad, C_h = 0.4×10^{-8} m^3/s Pa, and the instability index α_{vh} is 2.1 compared to the instability index α_v of 2.9 without the connecting hole but with the same simulation parameters. Because the first peak value of the rotary cylinder acceleration curve α'_{max} remains unchanged whether there is a connecting hole or not. In fact, α_{vh}/α_v is the ratio between the two maximum acceleration values with a connecting hole or without. From the ratio, we can see clearly that the connecting hole can relieve 25% of the acceleration peak value at the most.

5 Experimental Results

Now it's time to drill a connecting hole into the shaft of the rotary actuator with the specifications resulting from the GA (Fig. 8).

The same test bench in Fig. 1 was used as well as the modified rotary actuator to do the instability test mentioned above. Figures 9 and 10 illustrate the comparison of the test results between the original rotary actuator and modified rotary actuator which has the same test parameters.

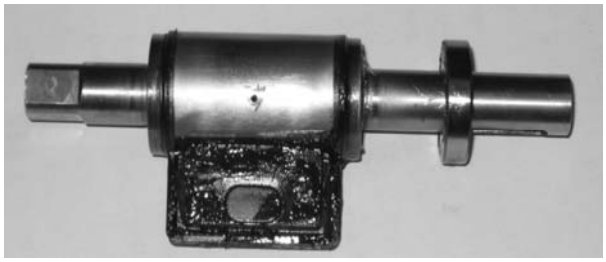

Fig. 8: *The shaft with drill hole*

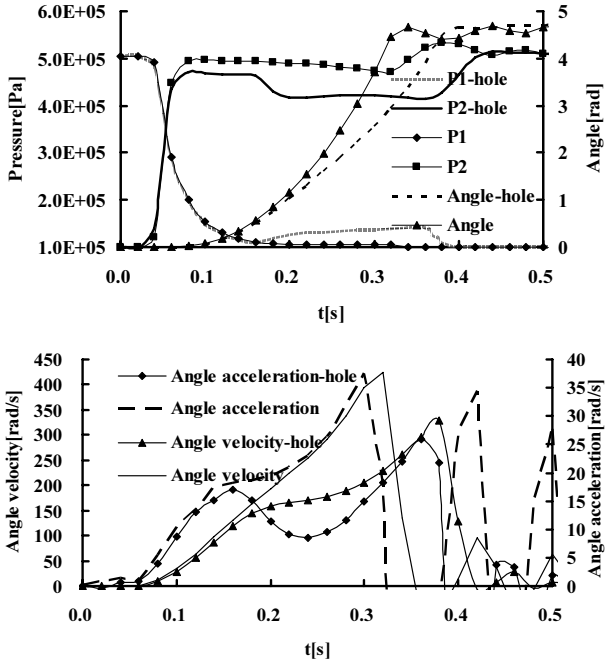

Fig. 9: *Comparison of the experimental results of the dynamic characteristics between the modified rotary actuator and the original rotary actuator (M_{ec} = 2.18 Nm, p_s = 0.4 MPa, θ_o = 0.5548 rad, θ_c = 4.1552 rad , C_h = 0.4×10^{-8} m^3/s Pa)*

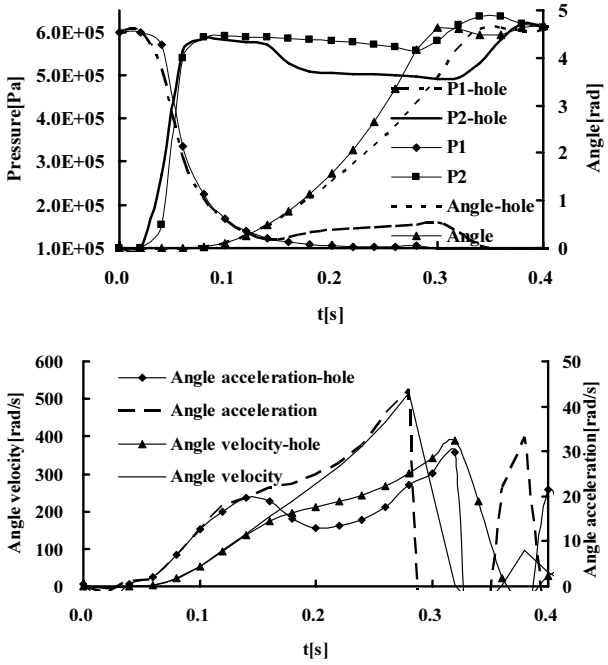

Fig. 10: *Comparison of the experimental results of the dynamic characteristics between the modified rotary actuator and the original rotary actuator (M_{ec} = 2.18 Nm, p_s = 0.5 MPa, θ_o = 0.5548 rad, θ_c = 4.1552 rad, C_h = 0.4×10^{-8} m^3/s.Pa)*

As illustrated in Fig. 9 the instability index α_v of original rotary actuator is equal to 2.75 and the instability index α_v of the modified rotary actuator is equal to 2.12. The ratio of maximum angular acceleration is about 0.72, that is to say, the modified rotary actuator can reduce the amplitude of maximum angular acceleration about 27%.

As illustrated in Fig. 10 the instability index α_v of the original rotary actuator is equal to 2.52 and the instability index α_v of the modified rotary actuator is equal to 1.6. The ratio of maximum angular acceleration is about 0.75, that is to say, the modified rotary actuator can reduce the amplitude of maximum angular acceleration about 25%.

According to Fig. 9 and Fig. 10, before the hole in the shaft of the rotary actuator is open at θ_o, the maximum torque generated by the rotary actuator is equal to that generated by the original rotary actuator. After that the maximum torque generated by the rotary actuator is reduced to about 84% of that generated by the original rotary actuator. The amount of air consumed rises to be 15% higher than that of the original rotary actuator.

The experimental results show that the method of the connecting hole is truly useful to reduce the eccentric load influence on the dynamic characteristics of the pneumatic rotary actuator. It can reduce the amplitude of maximum angular acceleration of the rotary actuator about 25%.

6 Conclusion

An experimental study has been performed to investigate the influence of eccentric loads on the dynamic characteristics of pneumatic rotary actuators mounted vertically, in which the instability index α_v was founded which provides an optimization object for the optimization design following.

An idea of increasing the back pressure by drilling a hole into the rotary shaft of the rotary cylinder which connects one working chamber to the other within a rotary angle range has been proposed.

To fulfill the design procedure of a connecting hole a mathematical model considering the connecting hole is built and its validity has been proved by comparison between simulation and experimental results.

Finally an optimization design based on the mathematical model above with the optimization object to minimize α_v is fulfilled. In the optimization the RGA optimization algorithm is used.

Both the simulation and experimental results prove that the method of the connecting hole is truly useful to reduce the eccentric load influence on the dynamic characteristics of the pneumatic rotary actuator.

Nomenclature

α_v	Stability index	
α'_{max}	First local maximum of rotary actuator acceleration	[rad/s^2]
α_{max}	Second local maximum of rotary actuator acceleration	[rad/s^2]
b	Critical pressure ratio	
C_1	Sonic conductance of chamber 1	[m^3/(s Pa)]
C_2	Sonic conductance of chamber 2	[m^3/(s Pa)]
C_h	Sonic conductance of connecting hole	[m^3/(s Pa)]
D	Inner diameter of rotary actuator	[m]
d	Diameter	[m]
g	Gravity acceleration	[m/s^2]
h	Thickness of the pane	[m]
hole	Modified rotary cylinder	
γ	Anglular acceleration	
J	Moment of inertia	[kg m^2]
k	Adiabatic coefficient	
l	Length	[m]
k_w	Viscosity damping coefficient	[Ns/m]
M	Load torque	[Nm]
M_{ec}	Eccentric load torque	[Nm]
m	Mass of gas	[kg]
p_1	Absolute pressure in chamber 1	[Pa]
p_2	Absolute pressure in chamber 2	[Pa]
p_s	Absolute supply pressure in chamber	[Pa]
p_a	Atmosphere pressure	[Pa]
q_{m1}	Mass flow rate into chamber 1	[kg/s]
q_{m2}	Mass flow rate out of chamber 1	[kg/s]
q_{mh}	Mass flow rate passing connecting hole	[kg/s]
R	Gas constant	[Nm/(kgK)]
ω	Angular velocity	[rad/s]
r	Distance between the blade edge and the rotary cylinder shaft	[m]
ρ_0	Air density under standard situation	[kg/m^3]
S	Angle of full stroke	[rad]
θ	Rotary angle	[rad]
θ_1	Rotary angle of chamber 1	[rad]
θ_2	Rotary angle of chamber 2	[rad]
θ_{1b}	Dead angle of chamber 1	[rad]
θ_{2b}	Dead angle of chamber 2	[rad]
θ_o	Opening angle	[rad]
θ_c	Closeing angle	[rad]
T_1	Temperature in chamber 1	[K]
T_2	Temperature in chamber 2	[K]
T_a	Temperatureof environment	[K]
T_0	Temperature in standard situation	[K]
T_s	Temperature of air source	[K]
t_e	Time to the end stroke	[s]
V_1	Volume of chamber 1	[m^3]
V_2	Volume of chamber 2	[m^3]
V_{1b}	Dead volume of chamber 1	[m^3]
V_{2b}	Dead volume of chamber 2	[m^3]

References

Li, J. F. 1991. Dynamics of pneumatic transmission system, *HuaNan institute of technology publish society*, WuHai.

Wang, L. 2003. On Nonlinear Constrained Optimization, *journal of liaoning institute of technology*, 23(1), pp. 13-15.

Wang, P., **Peng, G.** and **Wu, Q.** 2004. Application of parameter adjustors based on stability theory to pneumatic manipulators, *Journal of University of Science and Technology Beijing*, 26(6), pp. 666-669.

Wang, P., **Peng, G.-Z.** and **Wu, Q.-H.** 2003. Intelligent PID control of pneumatic rotary actuator angle servo system, *Journal of Beijing Institute of Technology (English Edition)*, 12(SUPPL), pp. 16-19.

Wang, P., **Peng, G.-Z.** and **Wu, Q.-H.** 2003. Pneumatic rotary actuator angle control system, *Journal of Beijing Institute of Technology (English Edition)*, 12(4), pp. 362-365.

Yamamoto, K., **Ishii, M.**, **Noborisaka, H.** and **Hyodo, K.** 2004. Stand alone wearable power assisting suit - Sensing and control systems, *Proceedings - IEEE International Workshop on Robot and Human Interactive Communication,* pp. 661-666.

Ye Q., **Meng G. X.**, **Yang L. H.** and **Xie W. H.** 2006. Speed Stability Criterion of the Rotary Cylinder with Eccentric Load, *Journal of ShangHai JiaoTong University*, 40(12), pp. 2089-2092.

Yoshimitsu, T. and **Yamamoto, K.** 2004. Development of a power assist suit for nursing work, *Proceedings of the SICE Annual Conference,* pp. 691-694.

Zhang, Y. A. and **Nishi, A. B.** 2003. Low-pressure air motor for wall-climbing robot actuation, *Mechatronics*, 13(4), pp. 377-392.

Zhang, Y. and **Nishi, A.** 1999. Robot actuation with low-pressure air-powered motors, *Advanced Robotics*, 13(1), pp. 59-74.

Zhang, X. E. 2003. Practical pneumatic technology nowadays. *Mechanic engineering publish society,* Beijing.

Ye Qian
Ye Qian is a lecturer at ShangHai JiaoTong University. He received his Ph. D. degree from Harbin industry University in 2002. One of his present research efforts involves the simulation and control of pneumatic systems and research on the flow-rate characteristics of pneumatic components.

Meng GuoXiang
Meng GuoXiang is a professor at ShangHai JiaoTong University. She received her Ph. D. degree from the University of Wisconsin-Madison in 1987. One of her present research efforts involves the simulation and control of pneumatic transmission systems.